Computational Biology and Chemistry 87 (2020) 107242

Contents lists available at ScienceDirect

Computational Biology and Chemistry

journal homepage: www.elsevier.com/locate/cbac

Short communication for targeting natural compounds against HER2 kinase domain as potential anticancer drugs applying pharmacophore based molecular modelling approaches- part 2

Shailima Rampogu[a], Gihwan Lee[a], Ravinder Doneti[b], Keun Woo Lee[a,b,*]

[a] Division of Life Science, Division of Applied Life Science (BK21 Plus), Plant Molecular Biology and Biotechnology Research Center (PMBBRC), Research Institute of Natural Science (RINS), Gyeongsang National University (GNU), 501 Jinju-daero, Jinju 52828, Republic of Korea
[b] Department of Genetics, University College of Science, Osmania University, Hyderabad 500007, Telangana, India

ARTICLE INFO

Keywords:
HER2
Breast cancer
Dual inhibitors
EGFR/HER2 inhibitors
Brain metastasis

ABSTRACT

Breast cancer is one of the common causes of death noticed in women globally. In order to find effective therapeutics, the current investigation has focussed on identifying candidate compounds for EGFR and HER2. Accordingly, the pharmacophore modelling approaches were adapted to identify two prospective compounds and were docked against the target 3RCD that is complexed with TAK-285 a known dual inhibitor. Focussing on the target 3RCD, our results have showed that the compounds have demonstrated a good binding affinity towards the target occupying the binding pocket. They have established key residue interactions with stable molecular dynamics simulation results. The Hit compounds have demonstrated a potential to penetrate the blood brain barrier thereby enriching their therapeutics towards breast cancer brain metastasis. Taken together, our findings propose two candidate compounds as EGFR/HER2 inhibitors that might serve as novel chemical spaces for designing and developing new inhibitors.

1. Introduction

Breast cancer (BC) is a widely known cancer noticed among women (Sun et al., 2017) and its metastatic form is highly responsible for majority of the deaths(Hsu and Hung, 2016). Broadly, the BC can be grouped into five subtypes (Hsu and Hung, 2016) with high rate of survival when detected only in the breast(Hsu and Hung, 2016). The receptor tyrosine kinases (RTKs) demonstrates a pivotal role in the biological processes(Hsu and Hung, 2016), including cancer progression(Butti et al., 2018). When the genes encoding RTKs undergo dysregulation of signals, aberrant mutations and expressions results in the generations of diseases including cancers(Du and Lovly, 2018)(Hsu and Hung, 2016). The 58 known RTKs are grouped into 20 subfamilies (Lemmon and Schlessinger, 2010) according to the kinase domain sequence(Yamaoka et al., 2018).

The human genome consists of nearly about 500 kinases demonstrating specificity towards serine/threonine or tyrosine (Jura et al., 2011), with several regulatory domains in a majority of the kinases. Nevertheless, they exhibit a strikingly conserved phosphorylation mechanism. This involves a group of common structural features located at the active site of the kinases (Jura et al., 2011). Structurally, the protein kinases consists of a small amino-terminal lobe and large carboxy-terminal lobe with conserved α-helices and β-strands (Roskoski, 2019). The small lobe predominantly consists of a five-stranded antiparallel β-sheet (β1–β5) along with regulatory αC-helix present in active or inactive orientations, while the large lobe is chiefly made up of α-helical consisting of eight conserved helices (αD–αI, αEF1, αEF2) along with four short conserved β-strands (β6–β9) (Roskoski, 2019).The small lobe bears a conserved glycine-rich (GxGxΦG) ATP-phosphate-binding loop or the P-loop sandwiched by the β1- and β2-strands. Adjacent to this lies a conserved valine (GxGxΦGxV) binding via hydrophobic bonds with the ATP's adenine base and several small molecule inhibitors (Roskoski, 2019). The catalytic loop residues of the large lobe take part in the transfer of phosphoryl group from ATP to the protein substrates (Roskoski, 2019).

Notably, the ErbB family that broadly belongs to RTKs, comprises of four subgroups, namely, EGFR (epidermal growth factor receptor, also known as ErbB1/HER1), ErbB2 (HER2), ErbB3 (HER3), and ErbB4 (HER4)(Wieduwilt and Moasser, 2008). All the four receptors have a cysteine-rich extracellular ligand binding site, a transmembrane

* Corresponding author at: Division of Life Science, Division of Applied Life Science (BK21 Plus), Plant Molecular Biology and Biotechnology Research Center (PMBBRC), Research Institute of Natural Science (RINS), Gyeongsang National University (GNU), 501 Jinju-daero, Jinju 52828, Republic of Korea.
E-mail address: kwlee@gnu.ac.kr (K. Woo Lee).

https://doi.org/10.1016/j.compbiolchem.2020.107242
Received 23 September 2019; Received in revised form 24 February 2020; Accepted 28 February 2020
Available online 28 February 2020
1476-9271/

lipophilic segment, and an intracellular domain possessing tyrosine kinase catalytic activity (Iqbal and Iqbal, 2014). Earlier reports have reported the key residues by a local spatial pattern (LSP) alignment algorithm after performing the structural analysis of different conformations and documented the presence of residues from the regulatory or R-spine (four non-consecutive hydrophobic residues) and the catalytic or C-spine (eight hydrophobic residues)(Roskoski, 2014). The inter/intramolecular residues of the ErbB family are as follows. The residues from R-spine of ErbB1 are Met766, Leu777, Phe856, His835 and Asp896 and the C-spine residues Val726, Ala743, Leu844, Val843, Val845, Leu798, Thr903 and Leu907 (Roskoski, 2014). The ErbB2 R-spine residues are Met774, Leu785, Phe864, His843 and Asp904 and the residues from C- spine are Val734, Ala751, Leu852, Val851, Val853, Leu806, Thr911 and Leu915. The ErbB3 has residues such as Ile763, Leu774, Phe853, His832 and Asp893 in R-spine and Val723, Leu841, Val840, Val842, Leu795, Thr900 and Leu904 in C- spine. Furthermore, the key residues in ErbB4 are Met772, Leu783, Phe862, His841 and Asp902 in R-spine and Val732, Ala749, Leu850, Val849, Val851, Leu804, Thr909 and Leu913 in C-spine (Roskoski, 2014).

EGFR is a well studied target in certain cancers such as colorectal cancer, squamous cell carcinoma and non-small cell lung cancer besides being involved with breast cancer (Guo et al., 2017). Additionally, it is reported that the expression of EGFR is elevated on the membranes of multidrug resistance (MDR) tumour cells (Jin et al., 2016). The gene HER2 is associated with 25–30 % of primary tumours resulting in enhanced cell proliferation, invasiveness, angiogenesis and decreased apoptosis (Jeon et al., 2017). HER2 is a non-ligand gene that requires dimerization with the ligand-bound receptors of the HER family (Jeon et al., 2017). One such partners for HER2 is EGFR both of which are in amplified levels in BC. Their corresponding dimerization promotes aggressive clinical behavior (Jeon et al., 2017).

Targeting EGFR/HER2 is an extensively studied strategy as anticancer treatment (Ghorab et al., 2018)(Yin et al., 2016) and certain chemical compounds have gained Food and Drug Administration (FDA) approval(Medina and Goodin, 2008). Moreover, mounting evidences report the designing and synthesis of such inhibitors to combat cancer (Yin et al., 2016)(Ghorab et al., 2018)(Sadek et al., 2014). In connection to this, the anilinoquinazoline derivatives were designed, synthesized and were further tested experimentally. The results have demonstrated that the aryl 2-imino-1,2-dihydropyridine derivatives were potential against both EFGR and HER2. They have displayed an IC_{50} equal to 2.09 and 1.94 μM on EGFR and 3.98 and 1.04 μM on HER2 (Sadek et al., 2014). Siyuan Yin etal., have designed and synthesized the inhibitors with oxazolo[4,5-*g*]quinazolin-2(1 H)-one scaffold. A majority of their compounds have presented moderate to high inhibitory activity against EGFR and HER2 (Yin et al., 2016). In another investigation, Mostafa et al., have designed and synthesized *N*-substituted-2-(4-oxo-3-(4-sulfamoylphenyl)-3,4-dihydrobenzo[*g*]quinazolin-2-ylthio) acetamides using 4- (2-mercapto -4-oxobenzo [g] quinazolin -3 (4 H) -yl) benzenesulfonamide as the starting material. All the compounds have rendered an IC_{50} spanning between 0.36–40.90 μM(Ghorab et al., 2018). More recently, an array of sulphonamide benzoquinazolinones were synthesized which have demonstrated potent activity on both EGFR and HER2 than erlotinib (Soliman et al., 2019). Recent studies illuminate the use of computational methods in designing dual inhibitors using comparative analysis of molecular interaction fields (CoMFA) and comparative molecular similarity index analysis (CoMSIA) (de Angelo et al., 2018). Besides these, Lapatinib, whose structure is represented in supplementary Fig. 1A, was the first dual inhibitor to gain approval from the U S Food and Drug Administration(FDA) in the year 2007(Medina and Goodin, 2008). Encouraged by these reports, the current research has employed several computational methods to retrieve compounds that could act as EGFR/HER2 inhibitors.

In this pursuit, in the previous investigation, two inhibitors (Hits) were identified by ligand-based pharmacophore modelling, virtual screening method and molecular dynamics simulation (MDS) studies (Rampogu et al., 2018). The target employed was EGFR kinase domain with the PDB code 3POZ in complex with TAK-285. In the current investigation, the identified Hits were assessed against the HER2 kinase domain 3RCD in complex with TAK-285. The compound TAK-285, whose structure is represented in supplementary Fig. 1B, is a dual inhibitor, that has demonstrated selective inhibition of HER2 and EGFR kinase activities(Doi et al., 2012). Therefore, the targets complexed with TAK-285 were selected for further evaluation. The objective of the current investigation is to evaluate the obtained Hits as potential HER2 inhibitors thereby, enriching their role as dual inhibitors.

2. Materials and methods

2.1. Selection of the protein and pharmacophore generation

The protein chosen for the present study is the HER2 kinase domain in complex with TAK-285 with the PDB code 3RCD(Ishikawa et al., 2011), which acts as a dual inhibitor for EGFR and HER2. Correspondingly, a structure-based pharmacophore was generated enabling the *Receptor Ligand Pharmacophore Generation* accessible with the Discovery Studio v18 (DS). This module promotes a set of pharmacophore models from the receptor ligand complex (Meslamani et al., 2012) complementary to the interactions. The ideal pharmacophore model was selected based upon the highest selectivity score that is predicted by a Genetic Function Approximation (GFA). During the execution of the protocol, the maximum pharmacophores was selected as 10, with minimum features as 4 and maximum features as 6, while retaining all the other specifications as default. The key residues were defined for all the residues around 10 Å (Ishikawa et al., 2011). Accordingly, the residues, Leu726, Gly727, Val734, Ala751, Lys753, Met774, Arg784, Leu785, Leu796, Thr798, Gln799, Leu800, Met801, Gly804, Cys805, Leu852, Thr862, Asp863, Phe864 and Phe1004 were labelled as key residues.

2.2. Validation of the generated pharmacophore model

The selected pharmacophore model was validated to assess its ability in redeeming the active compounds from a given dataset. The Güner-Henry (decoy set) method of validation was conducted with 190 small molecule (D) inhibitors specific to HER2 and were compiled as a dataset. This dataset consists of 40 active compounds (A) that have demonstrated an IC_{50} value below 2 nM. The remaining 150 compounds were considered as inactive compounds with the IC_{50} value above 10,000 nM. Subsequently, employing the formula for goodness of Hit list (GH) (Sakkiah et al., 2010)(Sakkiah and Lee, 2012), the efficiency of the pharmacophore was assessed.

$$GH = \left(\frac{Ha}{4HtA}\right)(3A+Ht)X\left\{1 - \frac{Ht- Ha}{D- A}\right\}$$

2.3. Mapping of the Hits onto the pharmacophore model

The two Hits identified from the previous research (Rampogu et al., 2018) were further mapped onto the generated pharmacophore model to comprehend on their key features necessary for a prospective dual inhibitors. Correspondingly, the *Ligand Pharmacophore Mapping* protocol was enabled electing the *best mapping only* as *True* with *fitting method* as *Rigid.* This fitting method ensures a rigid fit between the pharmacophore and the ligand. The other parameters were selected as default.

2.4. Molecular docking and molecular dynamics simulation studies

The two compounds were then assessed for their binding affinities with the protein 3RCD by docking them into the proteins active site.

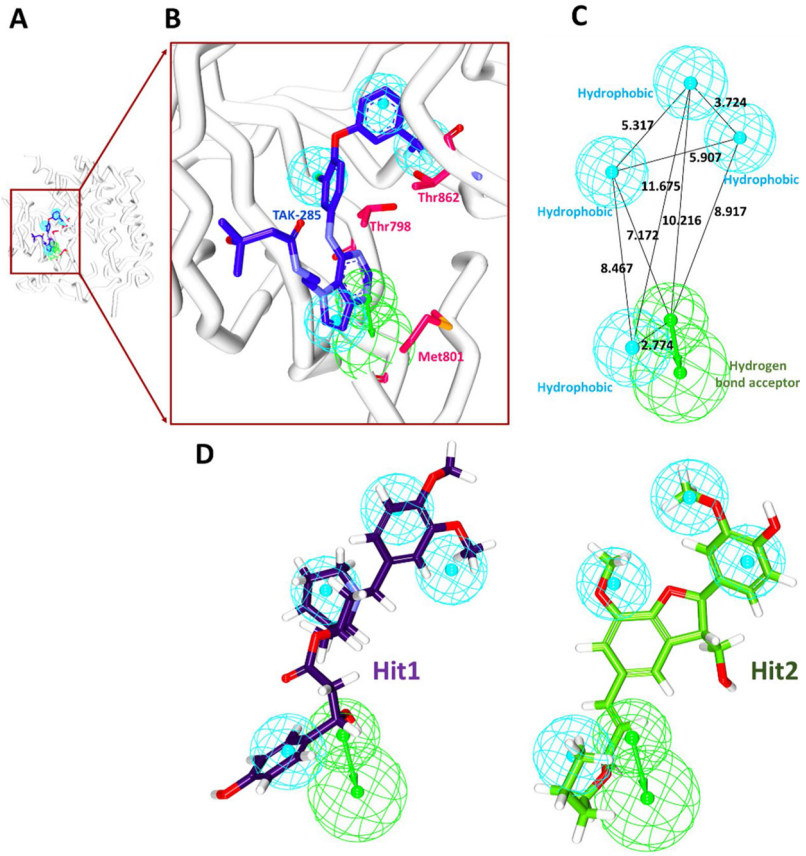

Fig. 1. Generation of structure-based pharmacophore model. A) Pharmacophore model corresponding to TAK-285. B) Key residues complementary to the pharmacophore features. C) Geometry between the pharmacophore features. D) Alignment of Hit1 and Hit2 onto the pharmacophore features.

Table 1
Pharmacophore summary illustrating different models and features.

Model	Number of Features	Feature Set	Selectivity Score
Model 1	5	HBA, HyP, HyP, HyP, HyP	8.1561
Model 2	4	HyP, HyP, HyP, HyP	6.6413
Model 3	4	HBA, HyP, HyP, HyP	6.6413
Model 4	4	HBA, HyP, HyP, HyP	6.6413
Model 5	4	HBA, HyP, HyP, HyP	6.6413
Model 6	4	HBA, HyP, HyP, HyP	6.6413

The protein was prepared by checking for gaps, removing the heteroatoms and water molecules after supplementing with the hydrogen atoms. The active site residues were plotted for all the atoms around the cocrystal at 10 Å by enabling the *Define and Edit Binding Site* module obtainable with DS. The CDOCKER (Wu et al., 2003) protocol available with the DS was employed with the generation of 100 conformations. The best pose was chosen based upon the dock score, read according to -CDOCKER interaction energy, prospective binding mode from the largest cluster and the key residue interactions.

The best-docked complexes were employed as initial structures for

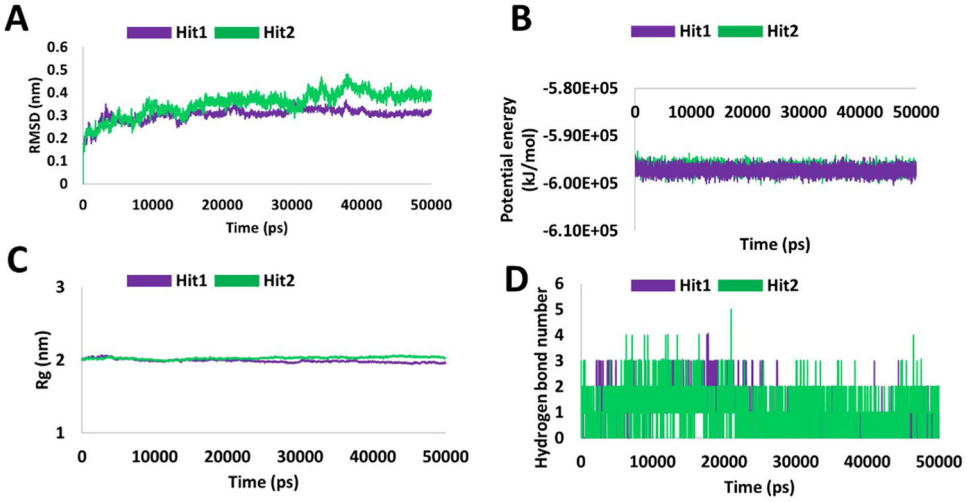

Fig. 2. Molecular dynamics simulation results. A) Backbone stability analysis. B) Plots indicating the potential energies of Hit1 and Hit2. C) Compactness of the protein by Rg. D) Enumerating the number of hydrogen bonds during 50 ns simulation run.

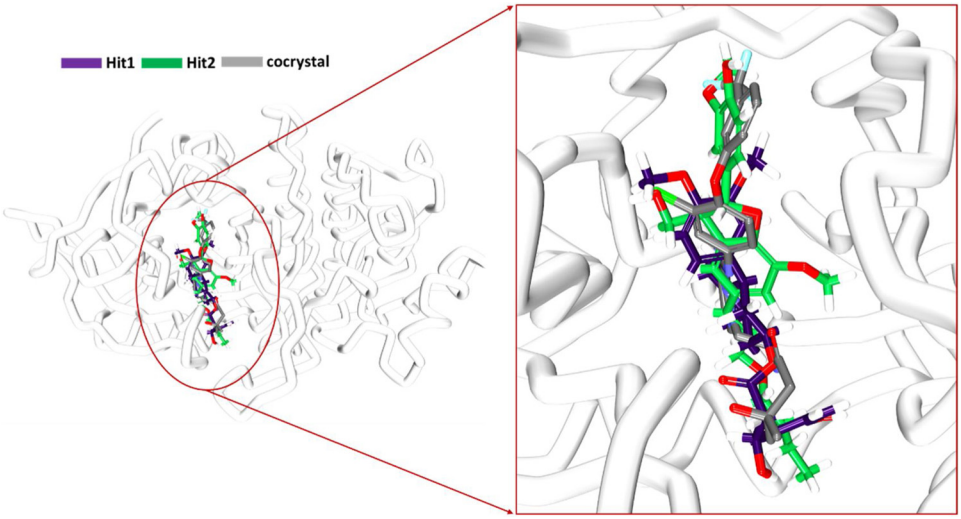

Fig. 3. Binding mode analysis of the Hit compounds. Accommodation of the Hits at the proteins active site in comparison with TAK-285.

molecular dynamics simulation (MDS) studies to assess the behaviour of the small molecules. The study was conducted using the CHARMM 27 all atom force field employing the GROningen MAchine for Chemical Simulations (Van Der Spoel et al., 2005) (GROMACS 2016.16), extracting the small molecule coordinates from SwissParam(Zoete et al., 2011). The simulations were carried out in a dodecahedron water box containing TIP3P water model and supplementing with the counter ions and subsequently energy minimized. A double step equilibration was conducted with (constant number of particles, volume, and temperature) NVT and (constant number of particles, pressure, and temperature) NPT ensembles. The NVT was conducted using V-rescale thermostat for 1 ns at 300 K, while the NPT was executed for 1 ns at 1 bar using Parrinello-Rahman barostat. Each ensemble was forwarded to MDS for 50 ns. The resultant findings were analysed employing the visual molecular dynamics (VMD)(Humphrey et al., 1996) and DS.

3. Results

3.1. Structure based pharmacophore generation

Exploiting the features of the crystal structure 3RCD and the co-crystallized ligand, a receptor-guided pharmacophore was generated. Correspondingly, six models were generated comprising of different features and selectivity scores as represented in Table 1. From the obtained models, the best model was chosen based upon the selectivity score and the number of features. The model 1 has represented five features with four hydrophobic (HyP) and hydrogen bond acceptor (HBA) along with a highest selectivity score of 8.1561. Upon thorough examination of the features, it was vivid that these features were complementary to the key residue. The HBA feature was complementary to the key residue Met801, while, hydrophobic bonds were complementary to the residues, such as Thr798 and Thr862, respectively as depicted in Fig. 1A and B. The 3D spatial relationship and distance constraints between these features are represented in Fig. 1C. Therefore, model 1 was chosen for further analysis.

3.2. Validation of the generated pharmacophore model

The selected pharmacophore was evaluated for its suitability in retrieving the active compounds when subjected to virtual screening against a larger dataset of compounds. Therefore, the model 1 was allowed to screen a dataset of 190 compounds with 40 active compounds in it. Upon enabling *Ligand Pharmacophore Mapping,* the model has mapped to 41 compounds (Ht) consisting of 40 active compounds (Ha). The goodness of Hit list was calculated as 0.95. These findings elucidate that the pharmacophore was efficient in retrieving the active compounds from the inactive compounds.

3.3. Evaluating the pharmacophore features of the compounds

The prospective compounds were assessed for possessing the important pharmacophore features by enabling the *Ligand Pharmacophore Mapping* tool accessible with the DS. The results have shown that the two compounds have mapped thoroughly with the pharmacophore model, Fig. 1D, inferring to be the active compounds.

3.4. Molecular docking and molecular dynamics simulation studies

Computational molecular docking is employed to delineate on the bimolecular interactions (Forli et al., 2016) to foretell the experimental binding modes of small molecules and estimate the binding affinities (Guedes et al., 2014). The two compounds were escalated to interact with the protein at its binding site employing the CDOCKER protocol. The results have shown that the Hits have demonstrated the -CDOCKER interaction energy of 63.66 kcal/mol and 59.22 kcal/mol were from the largest cluster. Additionally these compounds have shown various interactions with the key residues positioning the ligand at the active site.

To gain in-depth insight on the accommodation of prospective candidate compounds at the proteins active site, the molecular dynamics simulation studies were carried out (Liao et al., 2014) for 50 ns run. The stability of the systems was evaluated based upon the root mean square deviation (RMSD), potential energy and radius of gyration (Rg). The RMSD findings have deduced that the systems were stable demonstrating an RMSD around 0.4 nm. The average RMSD of Hit1 was calculated as 0.29 nm and Hit2 was recorded as 0.35 nm as illustrated in Fig. 2A. Additionally, both the systems have rendered stable potential energies throughout 50 ns simulation run as shown in Fig. 2B. The radius of gyration elucidates the compactness of the protein and the results have inferred by the Rg profiles revealed that the systems were compact, as illustrated in Fig. 2C.

Furthermore, the structures from last 5 ns were extracted to evaluate the binding modes of the Hits. Upon subsequent superimposition, it was noted that the Hits have occupied the same binding pocket as that of the cocrystallized ligand as depicted in Fig. 3. Upon scrupulous examination for the intermolecular interactions, it was observed that Hit1 has formed two hydrogen bond interactions with the residues Asp808 and Thr862 with an acceptable bond length as shown in Fig. 4A. The residues Val734, Ala751, Leu800, Cys805, and Leu852

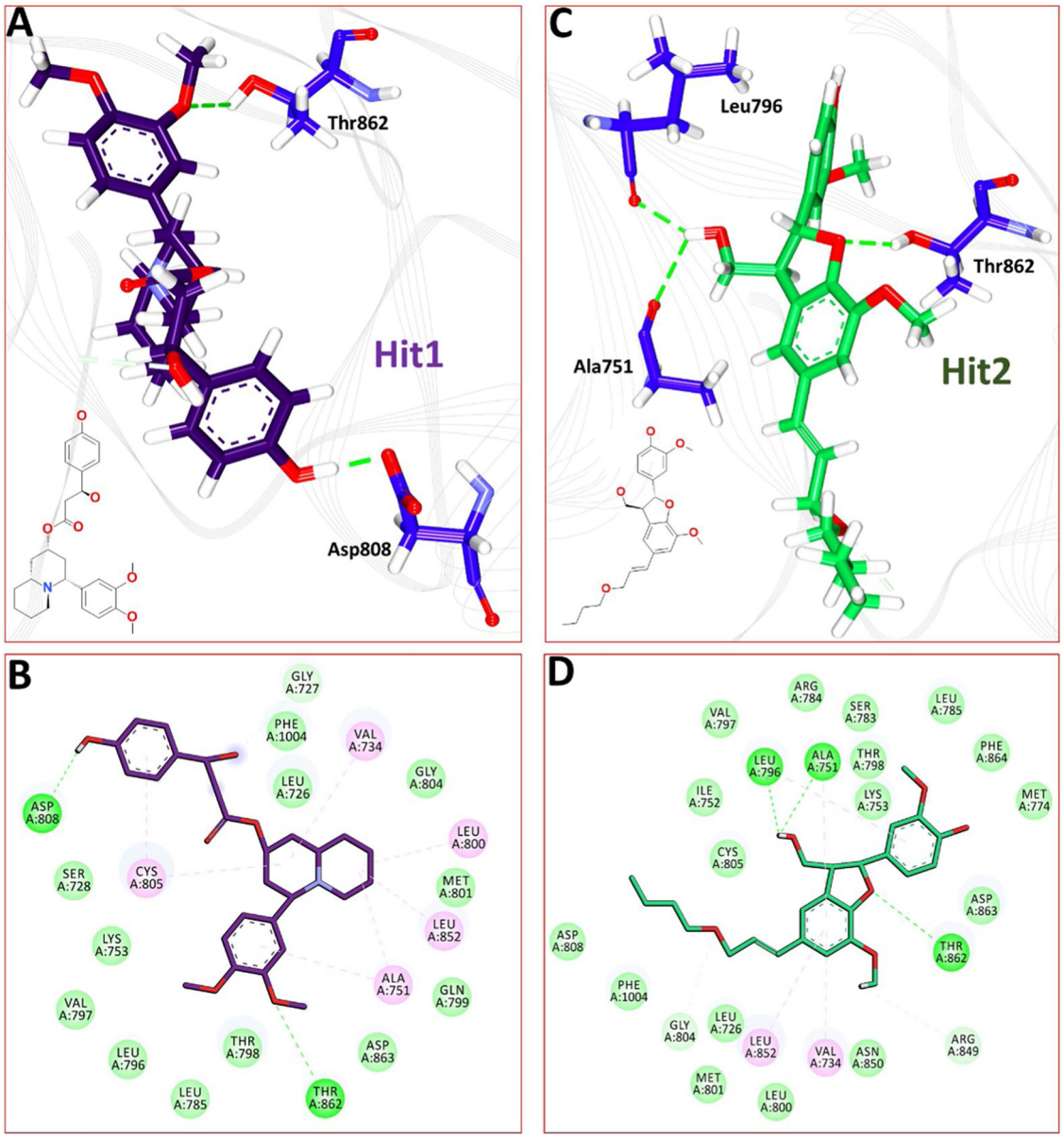

Fig. 4. Molecular interactions between the protein and the Hits. A) Depicts the hydrogen bond interactions between the active site residues and Hit1. B) Overall 2D interactions between Hit1 and the interacting residues. C) Interaction of Hit2 with the active site residues depicted by hydrogen bonds. D) 2D interactions between Hit2 and the residues. The hydrogen bond interactions are represented in green dotted lines. In the 2D interactions, the van der Waals interactions are represented in dark green balls and the alkyl and π-alkyl interactions are displayed in pink balls. The 2D structures of the Hit compounds are represented in panel A and C respectively.

have prompted alkyl and π- interactions assisting the ligand to be nestled at the binding pocket. The residue Gly727 has displayed carbon-hydrogen bond. The residues, Leu726, Ser728, Lys753, Leu785, Leu796, Val797, Thr798, Gln799, Asp863, Met801, Gly804 and Phe1004 have formed the van der Waals interactions aiding the ligand to be seated at the binding pocket as demonstrated in Table 2 and Fig. 4B.

The Hit2 has interacted with the protein by three residues such as Ala751, Leu796 and Thr862, respectively as depicted in Fig. 4C. Additionally the residues Val734, Ala751, Leu796 and Leu852 have held the ligand by π-alkyl interactions. The residues Gly804 and Arg849 have generated carbon-hydrogen bond. The residues Leu726, Ile752, Lys753, Met774, Ser783, Arg784, Leu785, Val797, Thr798, Leu800, Met801, Cys805, Asp808, Asn850, Asp863, Phe864 and Phe1004 have interacted by van der Waals interactions accommodating the ligand at the active site of the protein as represented in Table 2 and Fig. 4D. These results guide us to comprehend that the identified compounds might act as HER2 inhibitors. Additionally, it was noted that the Hit1 has interacted with the residues originating from R-spine and C-spine involving the residues such as Leu785 and Val734. The Hit2 has interacted with one R-spine residue, Leu785 and two key residues from the C-spine, Ala751 and Leu852. Leu852 has formed the alkyl/π-alkyl-interaction with the Hits, while, Leu785 has rendered van der Waals interaction with both the Hits. Interestingly, the residues Ala751 has involved via the π-interaction with Hit1 and formed hydrogen bond interaction with Hit2.

Furthermore, the hydrogen bond number was monitored during the simulations. Both the Hits have recorded the hydrogen bond interactions throughout the simulations. Notably, the Hit2 has projected higher number of interactions than Hit1 as illustrated in Fig. 2D. The average number of hydrogen bond interactions for Hit1 were recorded as 0.80 and Hit2 has shown an average number of hydrogen bonds of

Table 2
Various interactions prompted between the Hits and the protein.

Name	-CDOCKER interaction energy (kcal/mol)	Hydrogen bonds	π-interactions	Van der Waals interactions	Synthetic accessibility score
Hit1	63.66	Asp808:OD1-H36 (1.7 Å) Thr862:HG1 -O25 (2.8 Å)	Val734, Ala751, Leu800, Cys805, Leu852	Leu726, Gly727, Ser728, Lys753, Leu785, Leu796, Val797, Thr798, Gln799, Asp863, Met801, Gly804, Phe1004	4.54
Hit2	59.22	Ala751:O-H39 (3.0 Å) Leu796:O-H39 (2.2 Å) Thr862:HG1-O16 (2.4 Å)	Val734, Ala751, Leu796, Leu852	Leu726, Ile752, Lys753, Met774, Ser783, Arg784, Leu785, Val797, Thr798, Leu800, Met801, Gly804, Cys805,Asp808, Arg849, Asn850, Asp863, Phe864, Phe1004	4.63

1.14 respectively.

4. Discussion

With an aim of identifying a chemical compound that would act as dual inhibitor for both EGFR and HER2, the investigation was initiated considering the pharmacophore modelling approaches. In the previous work a ligand based pharmacophore modelling was conducted to generate a pharmacophore model, Supplementary Table 1. Two compounds were identified as potential candidate compounds towards EGFR target bearing the PDB code 3POZ (Rampogu et al., 2018) which is in complex with the dual inhibitor TAK-285. In order to establish the identified inhibitors as potential dual inhibitors, in the current investigation, those candidate compounds were assessed computationally with the HER2 target having the PDB code 3RCD employing the structure based pharmacophore modelling.

The Hits compounds have aligned well with the pharmacophore model, generated utilizing the cocrystallized ligand TAK-285. Additionally, the molecular docking results have shown that the Hits have demonstrated a good dock score comparable with the cocrystallized ligand. Subsequent MDS findings have demonstrated that the Hits were accommodated in the binding site throughout the simulations complemented by stable results. Upon docking the cocrystallized ligand into the proteins active site, it was noted that the docked pose has displayed a similar binding mode as that in the crystal structure, Supplementary Fig. 1A, with a dock score of 68.44 kcal/mol. Upon viewing the interactions, it was noticed that the residue Thr862 has formed with both the Hit compounds as was seen with the cocrystallized TAK-285 and its docked pose, Fig. 4 and Supplementary Fig. 1B. The residue Leu852 has formed π-σ interactions in the crystal structure and the docked pose; however in the Hits this residue has prompted alkyl and π-alkyl interactions, Fig. 4B and D. Additionally, the residue Phe1004 has formed van der Waals interaction with the TAK-285 as was seen with the Hit compounds. These results demonstrate that the identified compounds may act as HER2 inhibitors.

To understand if the Hit compounds could cross the blood brain barrier (BBB), aiding to treat the breast cancer brain metastasis, the ADMET analysis was conducted by enabling the *ADMET Descriptors* tool available on the DS. The predicted results have shown that the compounds have generated ADMET_BBB_Level as 2. This value demonstrates that the compounds have medium ability to penetrate across the blood brain barrier (Padariya et al., 2014). Accordingly, these Hits may be beneficial in treating breast cancer brain metastasis conditions.

Additionally, the synthetic accessibility of the Hit compounds was analysed. The ability to synthesize a compound is one of the fundamental aspects attributed to identify the Hits and can be estimated by synthetic accessibility score (Daina et al., 2017) (Ertl and Schuffenhauer, 2009). For the current study, the SwissADME was employed by using the SMILES of the Hits as an input. The synthetic accessibility score ranges between 1 (very easy) to 10 (very difficult). The Hit compounds have demonstrated a score of 4.54 and 4.63, as depicted in Table 2, for Hit1 and Hit2 respectively. These scores are close to 1 inferring that the compounds could be easily synthesized.

5. Conclusion

In the current investigation, the two Hit compounds were evaluated computationally as prospective HER2 inhibitors. These inhibitors have rendered comparable dock scores with TAK-285 together with stable MDS results. Additionally, the Hits have resided at the active site of the protein throughout 50 ns simulation run. Furthermore, the computational predictions have also illuminated that Hits may also be employed to treat brain metastasis cases. Overall, our results proclaim that the Hits could act as novel dual EGFR/HER2 inhibitors and can serve as scaffolds for designing new compounds.

CRediT authorship contribution statement

Shailima Rampogu: Investigation, Methodology, Writing - original draft, Visualization. **Gihwan Lee:** Methodology, Writing - original draft. **Ravinder Doneti:** Investigation. **Keun Woo Lee:** Supervision, Validation, Funding acquisition.

Declaration of Competing Interest

The authors declare that they have no known competing of any kind.

Acknowledgement

This research was supported by the Bio & Medical Technology Development Program of the National Research Foundation (NRF) & funded by the Korean government (MSIT) (No. NRF-2018M3A9A7057263).

Appendix A. Supplementary data

Supplementary material related to this article can be found, in the online version, at doi:https://doi.org/10.1016/j.compbiolchem.2020.107242.

References

Butti, R., Das, S., Gunasekaran, V.P., Yadav, A.S., Kumar, D., Kundu, G.C., 2018. Receptor tyrosine kinases (RTKs) in breast cancer: signaling, therapeutic implications and challenges. Mol. Cancer 17, 34. https://doi.org/10.1186/s12943-018-0797-x.

Daina, A., Michielin, O., Zoete, V., 2017. SwissADME: a free web tool to evaluate pharmacokinetics, drug-likeness and medicinal chemistry friendliness of small molecules. Sci. Rep. https://doi.org/10.1038/srep42717.

de Angelo, R.M., Almeida, M., de, O., de Paula, H., Honorio, K.M., 2018. Studies on the dual activity of EGFR and HER-2 inhibitors using structure-based drug design techniques. Int. J. Mol. Sci. https://doi.org/10.3390/ijms19123728.

Doi, T., Takiuchi, H., Ohtsu, A., Fuse, N., Goto, M., Yoshida, M., Dote, N., Kuze, Y., Jinno, F., Fujimoto, M., Takubo, T., Nakayama, N., Tsutsumi, R., 2012. Phase I first-in-human study of TAK-285, a novel investigational dual HER2/EGFR inhibitor, in cancer patients. Br. J. Cancer 106, 666.

Du, Z., Lovly, C.M., 2018. Mechanisms of receptor tyrosine kinase activation in cancer. Mol. Cancer 17, 58. https://doi.org/10.1186/s12943-018-0782-4.

Ertl, P., Schuffenhauer, A., 2009. Estimation of synthetic accessibility score of drug-like molecules based on molecular complexity and fragment contributions. J. Cheminform. https://doi.org/10.1186/1758-2946-1-8.

Forli, S., Huey, R., Pique, M.E., Sanner, M.F., Goodsell, D.S., Olson, A.J., 2016. Computational protein-ligand docking and virtual drug screening with the AutoDock suite. Nat. Protoc. https://doi.org/10.1038/nprot.2016.051.

Ghorab, M.M., Alsaid, M.S., Soliman, A.M., 2018. Dual EGFR/HER2 inhibitors and apoptosis inducers: new benzo[g]quinazoline derivatives bearing benzenesulfonamide as anticancer and radiosensitizers. Bioorg. Chem. https://doi.org/10.1016/j.bioorg.2018.07.015.

Guedes, I.A., de Magalhães, C.S., Dardenne, L.E., 2014. Receptor-ligand molecular docking. Biophys. Rev. 6, 75–87. https://doi.org/10.1007/s12551-013-0130-2.

Guo, P., Pu, T., Chen, S., Qiu, Y., Zhong, X., Zheng, H., Chen, L., Bu, H., Ye, F., 2017. Breast cancers with EGFR and HER2 co-amplification favor distant metastasis and poor clinical outcome. Oncol. Lett. 14, 6562–6570. https://doi.org/10.3892/ol.2017.7051.

Hsu, J.L., Hung, M.C., 2016. The role of HER2, EGFR, and other receptor tyrosine kinases in breast cancer. Cancer Metastasis Rev. https://doi.org/10.1007/s10555-016-9649-6.

Humphrey, W., Dalke, A., Schulten, K., 1996. VMD: visual molecular dynamics. J. Mol. Graph. 14, 33–38. https://doi.org/10.1016/0263-7855(96)00018-5.

Iqbal, N., Iqbal, N., 2014. Human Epidermal Growth Factor Receptor 2 (HER2) in Cancers: Overexpression and Therapeutic Implications. Mol. Biol. Int. 2014, 1–9. https://doi.org/10.1155/2014/852748.

Ishikawa, T., Seto, M., Banno, H., Kawakita, Y., Oorui, M., Taniguchi, T., Ohta, Y., Tamura, T., Nakayama, A., Miki, H., Kamiguchi, H., Tanaka, T., Habuka, N., Sogabe, S., Yano, J., Aertgeerts, K., Kamiyama, K., 2011. Design and synthesis of novel human epidermal growth factor receptor 2 (HER2)/epidermal growth factor receptor (EGFR) dual inhibitors bearing a pyrrolo[3,2-d]pyrimidine scaffold. J. Med. Chem. https://doi.org/10.1021/jm2008634.

Jeon, M., You, D., Bae, S.Y., Kim, S.W., Nam, S.J., Kim, H.H., Kim, S., Lee, J.E., 2017. Dimerization of EGFR and HER2 induces breast cancer cell motility through STAT1-dependent ACTA2 induction. Oncotarget. https://doi.org/10.18632/oncotarget.10843.

Jin, Y., Zhang, W., Wang, H., Zhang, Z., Chu, C., Liu, X., Zou, Q., 2016. EGFR/HER2 inhibitors effectively reduce the malignant potential of MDR breast cancer evoked by P-gp substrates in vitro and in vivo. Oncol. Rep. https://doi.org/10.3892/or.2015.4444.

Jura, N., Zhang, X., Endres, N.F., Seeliger, M.A., Schindler, T., Kuriyan, J., 2011. Catalytic control in the EGF receptor and its connection to general kinase regulatory mechanisms. Mol. Cell. https://doi.org/10.1016/j.molcel.2011.03.004.

Lemmon, M.A., Schlessinger, J., 2010. Cell signaling by receptor tyrosine kinases. Cell 141, 1117–1134. https://doi.org/10.1016/j.cell.2010.06.011.

Liao, K.H., Chen, K.-B., Lee, W.-Y., Sun, M.-F., Lee, C.-C., Chen, C.Y.-C., 2014. Ligand-based and structure-based investigation for alzheimer's disease from traditional chinese medicine. Evid. Based Complement. Alternat. Med. 2014, 364819. https://doi.org/10.1155/2014/364819.

Medina, P.J., Goodin, S., 2008. Lapatinib: a dual inhibitor of human epidermal growth factor receptor tyrosine kinases. Clin. Ther. https://doi.org/10.1016/j.clinthera.2008.08.008.

Meslamani, J., Li, J., Sutter, J., Stevens, A., Bertrand, H.O., Rognan, D., 2012. Protein-ligand-based pharmacophores: generation and utility assessment in computational ligand profiling. J. Chem. Inf. Model. https://doi.org/10.1021/ci300083r.

Padariya, M., Kalathiya, U., Baginski, M., 2014. Docking simulations, molecular properties and admet studies of novel chromane-6,7-diol analogues as potential inhibitors of mushroom tyrosinase. Gene Ther. Mol. Biol.

Rampogu, S., Son, M., Baek, A., Park, C., Rana, R.M., Zeb, A., Parameswaran, S., Lee, K.W., 2018. Targeting natural compounds against HER2 kinase domain as potential anticancer drugs applying pharmacophore based molecular modelling approaches. Comput. Biol. Chem. 74, 327–338. https://doi.org/10.1016/j.compbiolchem.2018.04.002.

Roskoski, R., 2014. The ErbB/HER family of protein-tyrosine kinases and cancer. Pharmacol. Res. https://doi.org/10.1016/j.phrs.2013.11.002.

Roskoski, R., 2019. Properties of FDA-approved small molecule protein kinase inhibitors. Pharmacol. Res. https://doi.org/10.1016/j.phrs.2019.03.006.

Sadek, M.M., Serrya, R.A., Kafafy, A.H.N., Ahmed, M., Wang, F., Abouzid, K.A.M., 2014. Discovery of new HER2/EGFR dual kinase inhibitors based on the anilinoquinazoline scaffold as potential anti-cancer agents. J. Enzyme Inhib. Med. Chem. https://doi.org/10.3109/14756366.2013.765417.

Sakkiah, S., Lee, K.W., 2012. Pharmacophore-based virtual screening and density functional theory approach to identifying novel butyrylcholinesterase inhibitors. Acta Pharmacol. Sin. 33, 964–978. https://doi.org/10.1038/aps.2012.21.

Sakkiah, S., Thangapandian, S., John, S., Kwon, Y.J., Lee, K.W., 2010. 3D QSAR pharmacophore based virtual screening and molecular docking for identification of potential HSP90 inhibitors. Eur. J. Med. Chem. https://doi.org/10.1016/j.ejmech.2010.01.016.

Soliman, A.M., Alqahtani, A.S., Ghorab, M., 2019. Novel sulphonamide benzoquinazolinones as dual EGFR/HER2 inhibitors, apoptosis inducers and radiosensitizers. J. Enzyme Inhib. Med. Chem. https://doi.org/10.1080/14756366.2019.1609469.

Sun, Y.-S., Zhao, Z., Yang, Z.-N., Xu, F., Lu, H.-J., Zhu, Z.-Y., Shi, W., Jiang, J., Yao, P.-P., Zhu, H.-P., 2017. Risk factors and preventions of breast Cancer. Int. J. Biol. Sci. 13, 1387–1397. https://doi.org/10.7150/ijbs.21635.

Van Der Spoel, D., Lindahl, E., Hess, B., Groenhof, G., Mark, A.E., Berendsen, H.J.C., 2005. GROMACS: fast, flexible, and free. J. Comput. Chem. https://doi.org/10.1002/jcc.20291.

Wieduwilt, M.J., Moasser, M.M., 2008. The epidermal growth factor receptor family: biology driving targeted therapeutics. Cell. Mol. Life Sci. 65, 1566–1584. https://doi.org/10.1007/s00018-008-7440-8.

Wu, G., Robertson, D.H., Brooks, C.L., Vieth, M., 2003. Detailed analysis of grid-based molecular docking: a case study of CDOCKER - A CHARMm-based MD docking algorithm. J. Comput. Chem. https://doi.org/10.1002/jcc.10306.

Yamaoka, T., Kusumoto, S., Ando, K., Ohba, M., Ohmori, T., 2018. Receptor tyrosine kinase-targeted Cancer therapy. Int. J. Mol. Sci. https://doi.org/10.3390/ijms19113491.

Yin, S., Tang, C., Wang, B., Zhang, Y., Zhou, L., Xue, L., Zhang, C., 2016. Design, synthesis and biological evaluation of novel EGFR/HER2 dual inhibitors bearing a oxazolo[4,5-g]quinazolin-2(1H)-one scaffold. Eur. J. Med. Chem. 120, 26–36. https://doi.org/10.1016/j.ejmech.2016.04.072.

Zoete, V., Cuendet, M.A., Grosdidier, A., Michielin, O., 2011. SwissParam: a fast force field generation tool for small organic molecules. J. Comput. Chem. 32, 2359–2368. https://doi.org/10.1002/jcc.21816.